Spherical Cellulose–Nickel Powder Composite Matrix Customized for Expanded Bed Application

Hai-Feng Xia, Dong-Qiang Lin, Shan-Jing Yao

Department of Chemical and Biochemical Engineering, Zhejiang University, Hangzhou 310027, China

Received 22 June 2006; accepted 1 August 2006
DOI 10.1002/app.25629
Published online in Wiley InterScience (www.interscience.wiley.com).

ABSTRACT: Expanded bed adsorption (EBA) is an integrated technology for capturing target biomolecules directly from particle-containing feedstock. The adsorbents are the key base to achieve the EBA process and should be designed specially. In present work a new type of composite particles for EBA application was prepared with cellulose as the skeleton, and nickel powder as the densifier through the method of water-in-oil suspension thermal regeneration. Two fractions of spherical particles with mean sizes of 101–119 μm and 168–217 μm were obtained and the effects of nickel powder addition on the physical properties of composite particles were analyzed. The results indicated that the cellulose–nickel powder composite particles prepared have appropriate wet density of 1.14–1.78 g/mL, water content of 51–75%, porosity of 81–93%, pore radius of 41–59 nm, and specific surface area of 30–42 m^2/mL of wet particles. The bed expansion factor at the range of 2–3 was investigated and correlated with Richardson–Zaki equation. In addition, the bed stability with composite particles prepared was demonstrated with the observation of liquid mixing in expanded bed. © 2007 Wiley Periodicals, Inc. J Appl Polym Sci 104: 740–747, 2007

Key words: matrix; adsorption; hydrogels; composite particles; expanded bed adsorption; cellulose; nickel powder

INTRODUCTION

Expanded bed adsorption (EBA) was developed as an innovative chromatographic technique, allowing the adsorption of target proteins directly from unclarified feedstock, such as culture suspensions, cell homogenates, or crude extracts, without the need for prior removal of suspended solids. EBA technology integrates solid-liquid separation, concentration and primary purification into a single unit operation, aiming at increased overall recovery yield, reduced operational time, as well as less requirements for capital investment and consumables. The feasibility of this technique has been proven with a variety of expression systems (*E. coli*, yeast and mammalian cells).[1–4] Most important property of EBA is the perfectly classified fluidization of adsorbent.[5] Normally, a proper fluid velocity is chosen for the expansion factor at the range of 2–3, which could avoid particle-containing feedstock blocking the bed and keep the bed stable. To achieve this purpose, the adsorbents with certain density and size distribution should be designed specially. According to the application of EBA for large-scale bio-product separation, the prefect adsorbent trends to be small size, large pore, and high density. The small size and enlarged pore in the particles would reduce the pore diffusion and result in increasing the dynamic adsorption capacity. The adsorbent with high density would be suitable to high flow velocity and result in reducing the processing time.

In 1990s, Streamline series of adsorbents were developed by Amersham Biosciences and introduced to the market based on the demand of biotechnology industry. These adsorbents are based on 6% cross-linked agarose containing a crystalline quartz core as the densifier, with particle size at the range of 100–300 μm, and the mean density about 1.2 g/mL. Streamline adsorbents can be used under the fluid velocity of 200–400 cm/h in water corresponding to a suitable expansion factor of 2–3.[6] Currently, GE Healthcare developed a new adsorbent named Streamline Direct CST-1,[6] which is densified with stainless steel power and has the mean density of 1.8 g/mL. The particle size is in the range of 80–165 μm and the operation fluid velocity of 400–800 cm/h causes the expansion factor of 2–3. The materials and physical-chemical properties of adsorbent matrix determine the performance of EBA. During past 15 years, some research groups and companies have developed new series of matrices for EBA, such as agarose–crystalline quartz, agarose–stainless steel, agarose-Nd-Fe-B alloy,[7] agarose–tungsten carbide,[8] cellulose–titanium oxide,[9] cellulose–stainless steel,[10,11] etc. These adsorbents show some application prospect in the lab and industry. However, new series of adsorbents are still hoped for the perfect performance of EBA.

Base on the previous work,[10,11] a new type of cellulose-nickel composite particles were prepared with the method of water-in-oil suspension thermal regeneration in the present work. Cellulose is one of the most

Correspondence to: S.-J. Yao (yaosj@zju.edu.cn).

Journal of Applied Polymer Science, Vol. 104, 740–747 (2007)

widely used materials in packed bed chromatography.[12] The nickel powder was used as the densifier with the density of 8.9 g/cm^3 and mean size of 1.49 μm, which is stable in normal environment because of the compact oxide layer. Furthermore, nickel is a kind of magnetic material, which causes the prepared composite particles can also be used in the magnetic stabilization mode. The physical properties of the composite particles were studied and analyzed. The influence of densifier addition on the adsorbent density, water content, porosity, pore radius, and specific surface area was discussed. The expansion property and the liquid mixing in expanded bed were also analyzed for demonstrating the potential EBA application.

EXPERIMENTAL

Materials

Degreasing cotton was purchased from Jiaozuo League Health Material (Jiaozuo, China). Nickel powder with a density of 8.9 g/cm^3 and a mean particle diameter of 1.498 μm was ordered from Ningbo Guangbo Nano-Materials (Ningbo, China). A photograph of the powder is shown in Figure 1. Vacuum oil HFV-250 was purchased from Shanghai Huifeng Petrochemical (Shanghai, China). Streamline Direct CST-1 was a kind gift from GE Healthcare (Uppsala, Sweden). All other reagents were of analytical reagent grade from the local store.

Preparation of composite particles

The cellulose xanthate viscose was prepared as follows. 80 g crumbled degreasing cotton was treated by 18% (w/w) NaOH and aged in the air for 48 h, and then reacted with 50 mL CS_2 and dissolved in 6% (w/w) NaOH. The operations were under 15°C. The nickel powder densified composite particles were prepared through the method of water-in-oil suspension thermal regeneration as described in the previous work.[12] Generally, 100 g viscose mixed with a series of different amount of nickel powder (the weight ratio of Ni-powder to viscose: 1/10,1/8,1/6,1/4,1/3, and 1/2), and then the mixture was dispersed in 600 g vacuum oil in a 1 L flask with the agitation at 800–1000 rpm for 20 min at room temperature. The suspension was heated to 95°C, kept for 1.5 h under continuous stirring, and then cooled and filtered. The resulting particles were washed in turn with boiling water and ethanol for three times, and then dipped in acetic acid (25%, w/w) for 1 h. The particles were screened by standard sieves to two size ranges, 50–150 μm and 125–250 μm, named as Cell-Ni-S and Cell-Ni-L, respectively. Based on the amount of nickel powder in the composite particles, the small fractions were named Cell-Ni-S1 to Cell-Ni-S6, and the large fractions Cell-Ni-L1 to Cell-Ni-L6.

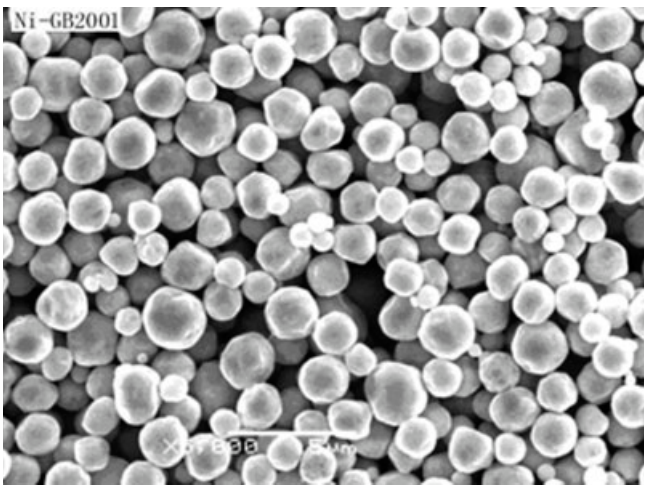

Figure 1 Photographs of nickel powder appearance and size.

Physical properties

The size distribution of the prepared composite particles was determined with the laser particle size analyzer Mastersizer 2000 (Malvern Instruments, Worcestershire, UK). The shape of the particles was observed by microscope Nikon E200 (Nikon Instruments, Japan).

The wet density (ρ_p, g/mL wet particles) was determined by water replacement in a 5 mL gravity bottle. Water content ω was obtained by dehydration at 120°C to a constant mass. Presuming that all pores in particles were full of water, porosity P (%) expressing pore volume per volume wet particles and pore volume V (ml/g dry particle) expressing pore volume per gram dried particles can be roughly estimated as follows, in which ρ_w represents the density of water,

$$P = \frac{\rho_p \omega}{\rho_w \times 100\%} \quad (1)$$

$$V = \frac{\omega}{(1-\omega)\rho_w} \quad (2)$$

Specific surface area S (m^2/mL) was obtained by adsorption of methylene blue solution and calculated as follow,[13]

$$S = \frac{(C_0 - C)G\rho_p}{m_p} \times 2.45 \quad (3)$$

where C_0 and C represent the initial and equilibrium concentrations of methylene blue solution, G and m_p represent the masses of methylene blue added and sample particles, respectively. The constant of 2.45 (m^2/mg methylene blue) means that 1 mg methylene blue could cover the area of 2.45 m^2 for the assumption of mono-molecule-layer adsorption.

According to the cylindrical pore structural model,[14] the mean pore radius R (nm) can be estimated as,

$$R = 2 \times 1000 \times \frac{V(1-\omega)\rho_p}{S} \quad (4)$$

Expansion characteristics

A XK16/column (Amersham Biosciences, 1.6 cm diameter, 35 cm length) with the movable adapters was used, which could adjust the position of liquid outlet to the top of expanded bed. The fluid was transported using a peristaltic pump (Longer Precision Pump, Baoding, China). Proper column vertical alignment was assured in all experiments. The bed height was measured three times for each flow rate after the expansion equilibrium and was used to calculate the bed expansion factor E,

$$E = \frac{H}{H_0} \quad (5)$$

where H is the expanded bed height, and H_0 is the sedimented bed height. In the present work H_0 was 10 cm.

The Richardson-Zaki correlation equation[15] was used to describe the expansion characteristics as follows,

$$U = U_t \varepsilon'' \quad (6)$$

Thus the relation between the voidage of expanded bed (ε) with the superficial liquid velocity (U) could be determined by the terminal settling velocity of particle (U_t) and the expansion index (n). The value of ε was calculated with the following equation,

$$E = \frac{H}{H_0} = \frac{1-\varepsilon_0}{1-\varepsilon} \quad (7)$$

where the voidage of sedimented bed (ε_0) is usually assumed as 0.4.[16]

Descriptions of liquid mixing in expanded bed

The measurement of residence time distribution (RTD) was used to determine the liquid mixing as the literature.[17] In each test, 0.5 mL acetone solution (10%, w/w) was injected at the bottom inlet of the column and the output was detected by the UV detector (WellChrom fast scanning spectrophotometer K-2600, KNAUER, Berlin, Germany). The response signal was recorded with the recorder.

As used in many literatures,[5,17] the Bodenstein number (Bo) and the axial mixing coefficient (D_{ax}), were calculated to evaluate the liquid mixing in the expanded bed according to the RTD test.

The Bo number, which relating convective transport of liquid to dispersion, is defined as

$$Bo = \frac{UH}{D_{ax}\varepsilon} \quad (8)$$

and Bo can be calculated from the number of theoretical plates (N) as,

$$\frac{1}{N} = \frac{2}{Bo} + \frac{8}{Bo^2} \quad (9)$$

The N can be determined from RTD test as following,

$$N = 5.54 \times \left(\frac{t_R}{W_{1/2}}\right)^2 \quad (10)$$

where t_R represents the residence time and $W_{1/2}$ represents the half peak width of RTD response.

Thus, the D_{ax} can be determined with Eqs. (8)–(10).

RESULTS AND DISCUSSION

Preparation of the composite particles

One of important steps for preparing spherical cellulose particles is the preparation of cellulose xanthate

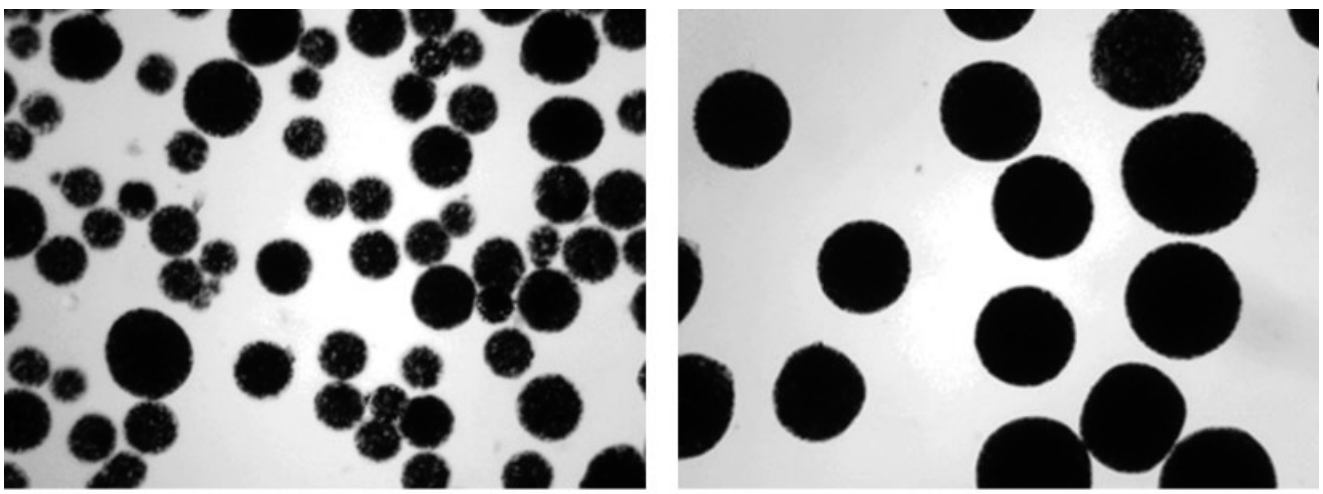

Figure 2 Photographs of particle appearance: (a) Cell-Ni-S; (b) Cell-Ni-L.

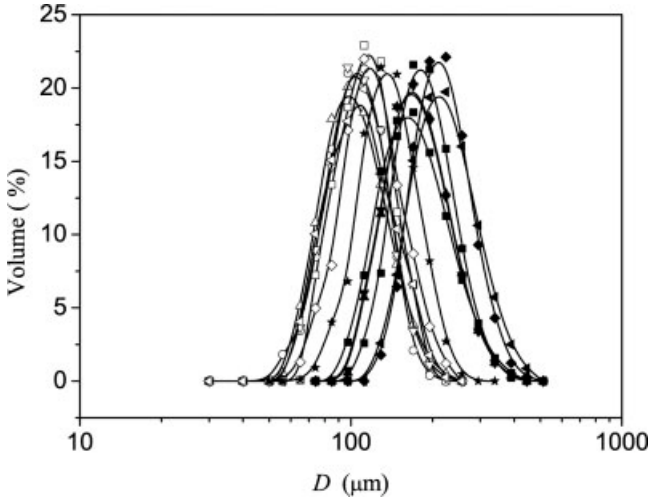

Figure 3 Size distributions of composite particles and streamline CST-1: □, Cell-Ni-S1; ○, Cell-Ni-S2; △, Cell-Ni-S3; ▽, Cell-Ni-S4; ◇, Cell-Ni-S5; ◁, Cell-Ni-S6; ■, Cell-Ni-L1; ●, Cell-Ni-L2; ▲, Cell-Ni-L3; ▼, Cell-Ni-L4; ◆, Cell-Ni-L5; ◀, Cell-Ni-L6; ★, streamline direct CST1.

viscose. According to the previous work,[11,12] the appropriate cellulose concentration in the viscose is about 7.5–8% (w/w), and the viscosity of viscose is at the range of 5000–8000 cSt. The alkali-treating, aging, and xanthating temperature and time should be controlled strictly in the process. In addition, it was found that the dispersing medium influenced the shape and size distribution of composite particles. Several operation conditions, including the types of dispersion oil, ratio of oil to viscose, and the surfactant added were investigated. To enhance the incompatibility of two phases, some amount of chlorobenzene was mixed in the vacuum oil (chlorobenzene : vacuum oil = 1 : 5), and 2 mL 30% (w/w) kalium oleate should be added in the flask before heating. The proportion of vacuum oil to the viscose was optimized as 6.

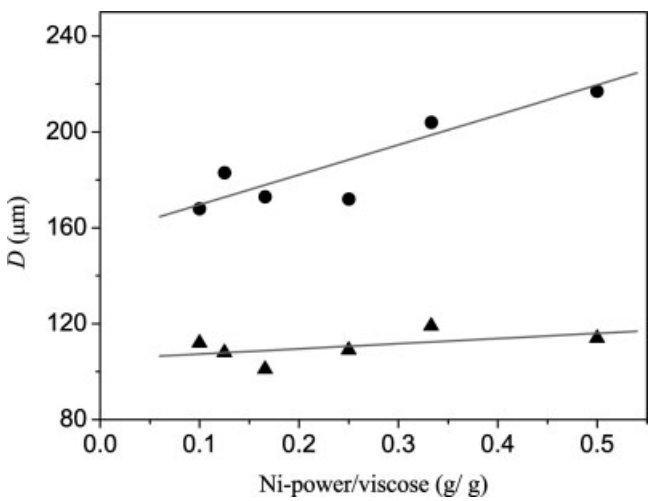

Figure 4 Effect of nickel content on the mean particle diameter for two size fractions: ▲, Cell-Ni-S; ●, Cell-Ni-L.

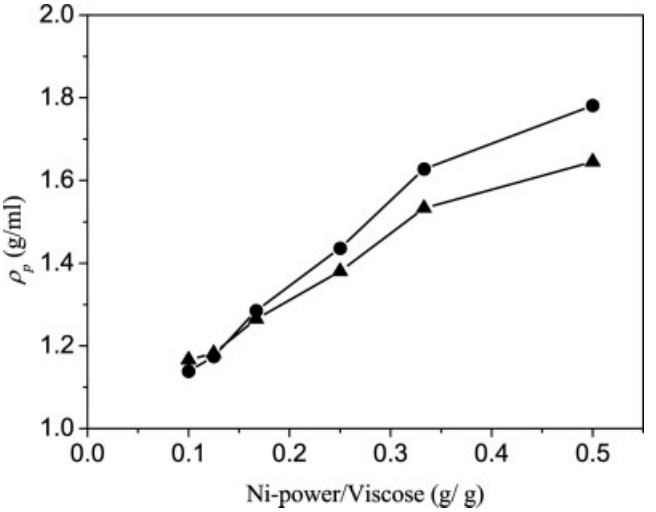

Figure 5 Particle wet densities of two size fractions for varying nickel content: ▲, Cell-Ni-S; ●, Cell-Ni-L.

For one batch, typically about 30% of composite particles were small size fractions (Cell-Ni-S), while the proportion of large fractions (Cell-Ni-L) was a little higher, about 40%. The others (about 30%) were larger than 250 μm. The result indicated that the composite particles prepared have a broad size distribution, and some amount of waste was unavoidable in this work.

Figures 2(a) and 2(b) give two samples of particle appearance. Figure 2(a) shows the appearance of Cell-Ni-S with small size and less nickel content, and Figure 2(b) shows the Cell-Ni-L with large size and relatively high nickel content. All fractions have the spherical shape and the crack and adhesion of particles were hardly found during the preparation.

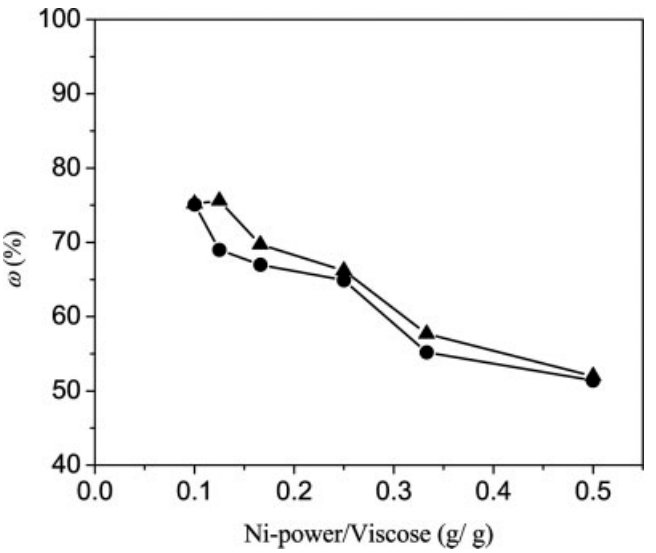

Figure 6 Water content of two fractions for varying nickel content: ▲, Cell-Ni-S; ●, Cell-Ni-L.

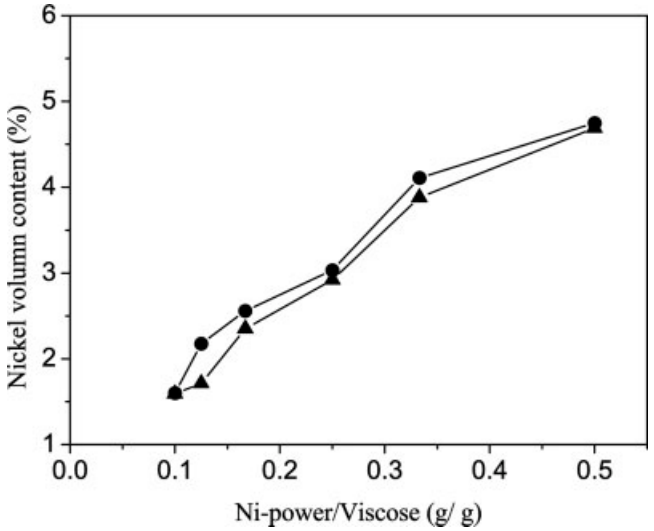

Figure 7 Nickel volume content of two fractions for varying nickel content: ▲, Cell-Ni-S; ●, Cell-Ni-L.

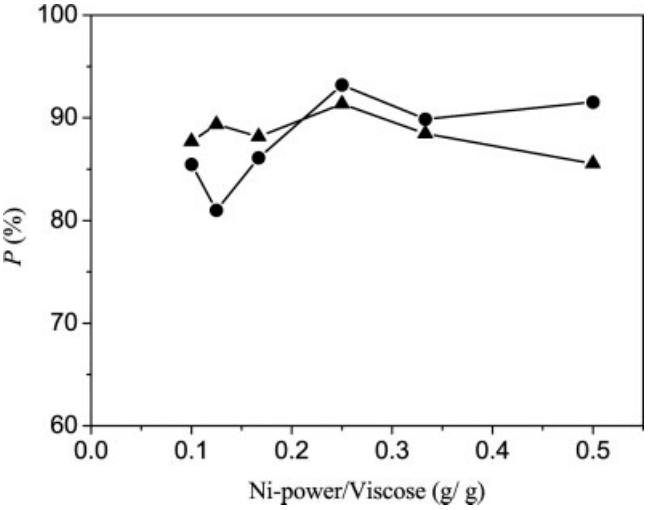

Figure 9 Porosity of two fractions for varying nickel content: ▲, Cell-Ni-S; ●, Cell-Ni-L.

Size distributions of composite particles

The size distributions of composite particles prepared were measured. Figure 3 shows the results with different nickel contents of two size fractions. It could be found that the size distributions of small fractions (Cell-Ni-S) were relatively similar to each other, while the large fractions (Cell-Ni-L) were discrepant with an obviously shift. All fractions have the logarithmic symmetrical distributions. Streamline Direct CST-1 was used as the comparison in the present work, and also showed a logarithmic symmetrical size distribution. The mean size of Streamline Direct CST-1 is about 130 μm, which is a little larger than the small fractions Cell-Ni-S. As shown in Figure 4, the mean particle sizes of small fractions were in the range of 101–119 μm, while the large fractions were 168–217 μm. The composite particles kept similar size for Cell-Ni-S and the mean particle diameters of Cell-Ni-L increased with the increase of nickel powder amount.

Particle wet density and water content

The operation fluid velocity for EBA application was determined by wet density of composite matrix, which could be controlled by the content of densifier in the particles. Figure 5 shows the effects of nickel content on the wet density of composite particles. With the increase of nickel content, the wet density of two fractions increased correspondingly. Normally, the wet density of Cell-Ni-L was higher than that of Cell-Ni-S. When the ratio of Ni-powder/viscose was 0.5, the wet density of two fractions could reach 1.65 and 1.78 g/mL, respectively.

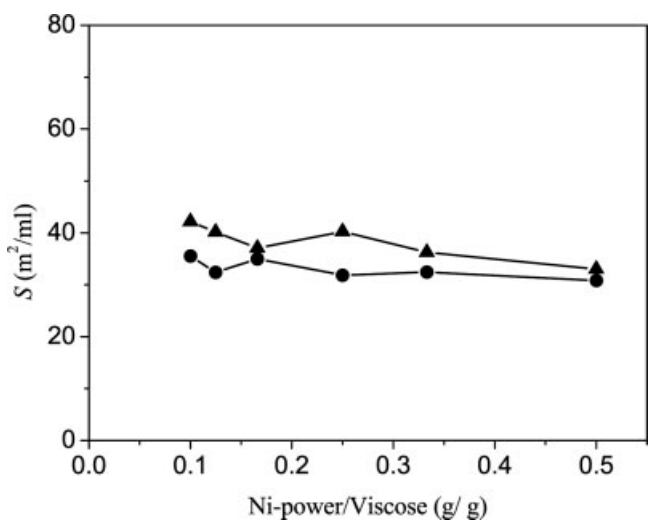

Figure 8 Special surface area of two fractions for varying nickel content: ▲, Cell-Ni-S; ●, Cell-Ni-L.

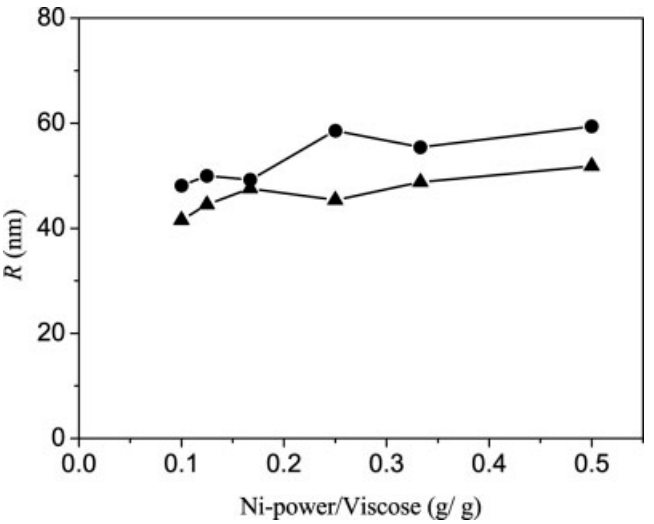

Figure 10 Mean pore radius of two fractions for varying nickel content: ▲, Cell-Ni-S; ●, Cell-Ni-L.

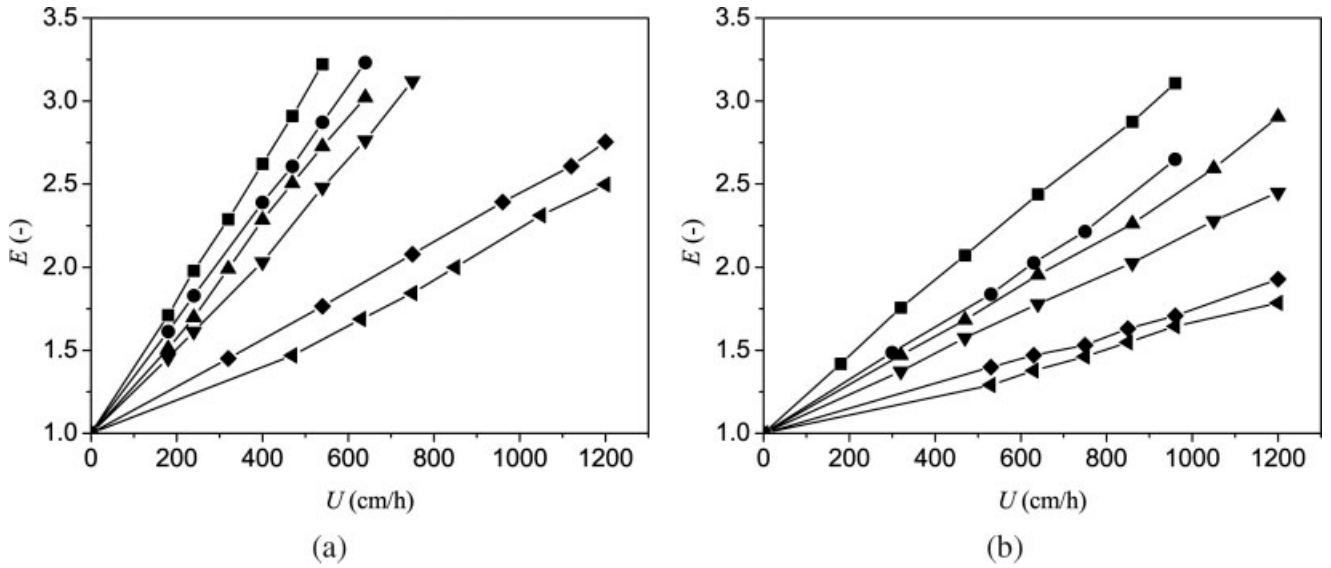

Figure 11 (a) Bed expansion of Cell-Ni-S for varying nickel content: ■, Cell-Ni-S1; ●, Cell-Ni-S2; ▲, Cell-Ni-S3; ▼, Cell-Ni-S4; ◆, Cell-Ni-S5; ◀, Cell-Ni-S6. (b) Bed expansion of Cell-Ni-L for varying nickel content: ■, Cell-Ni-L1; ●, Cell-Ni-L2; ▲, Cell-Ni-L3; ▼, Cell-Ni-L4; ◆, Cell-Ni-L5; ◀, Cell-Ni-L6.

The water content is another important property for the hydrophilicity and space capacity of the particles.[12] Figure 6 shows that water content in the composite particles decreased gradually with the increase of Ni-powder/viscose ratio. Based on the density and the water content, the nickel volume content in the particles could be calculated and the results are shown in Figure 7. It was found that the nickel volume content was less than 5% even when the Ni-powder/viscose ratio reached 0.5. The result indicates that the addition of Ni powder with high density has slight influence on the efficient volume of particle and the composite particles are suitable to use as the matrices for biomolecules separation.

Porous properties of composite particles

The effects of nickel content on the pore structure of composite particles are shown in Figures 8–10. Three important properties, including special surface area, porosity and mean pore radius, were investigated. It was found that the addition of nickel powder has less effect on the special surface area in the composite particles. The average value of special surface

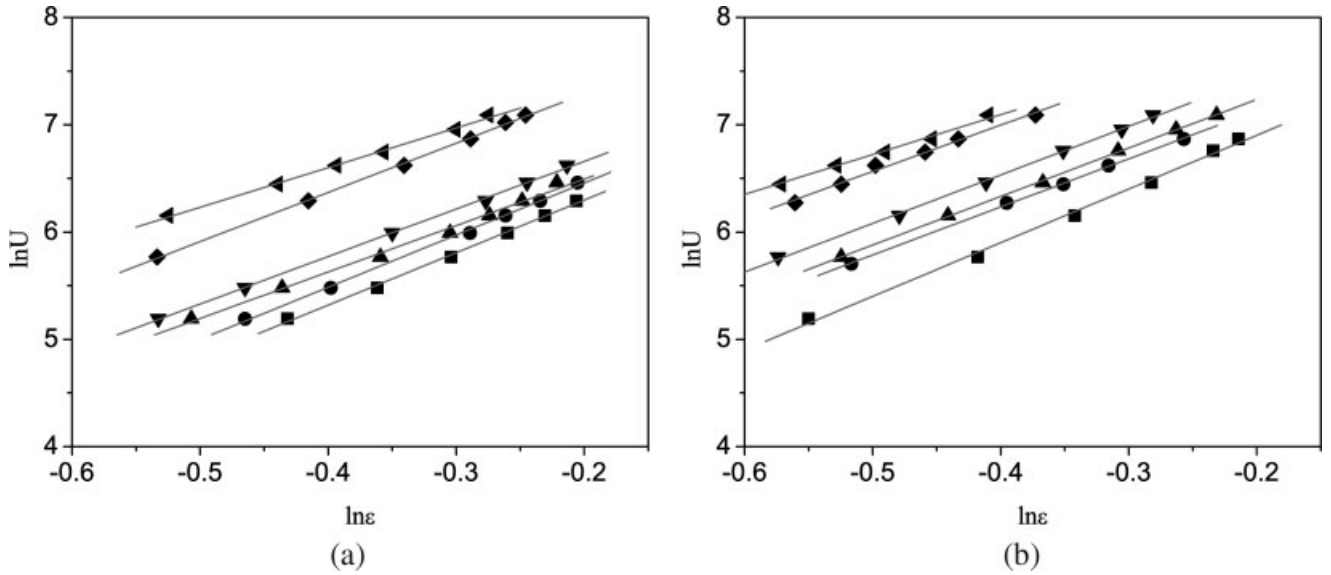

Figure 12 (a) Richardson-Zaki correlation with flow velocity and bed viodage: ■, Cell-Ni-S1; ●, Cell-Ni-S2; ▲, Cell-Ni-S3; ▼, Cell-Ni-S4; ◆, Cell-Ni-S5; ◀, Cell-Ni-S6. (b) Richardson-Zaki correlation with flow velocity and bed viodage: ■, Cell-Ni-L1; ●, Cell-Ni-L2; ▲, Cell-Ni-L3; ▼, Cell-Ni-L4; ◆, Cell-Ni-L5; ◀, Cell-Ni-L6.

TABLE I
Correlated Parameters with the Richardson–Zaki Equation for the Composite Particles

Matrix	U_t (cm/h)	n
Cell-Ni-S1	1444.3	4.89
Cell-Ni-S2	1684.7	4.86
Cell-Ni-S3	1570.6	4.33
Cell-Ni-S4	1890.2	4.43
Cell-Ni-S5	3659.0	4.59
Cell-Ni-S6	3225.4	3.70
Cell-Ni-L1	2703.9	5.00
Cell-Ni-L2	3061.4	4.48
Cell-Ni-L3	3431.4	4.52
Cell-Ni-L4	4197.7	4.52
Cell-Ni-L5	6185.0	4.33
Cell-Ni-L6	5325.3	3.72

area for Cell-Ni-S reached 38.16 m^2/mL, a little higher than that of Cell-Ni-L, 33.00 m^2/mL. The porosity of two fractions changed at the range of 85–92%. The mean pore radius of the composite particles reached the average values of 46.6 and 53.5 nm for Cell-Ni-S and Cell-Ni-L, respectively. The relatively large pore radius could greatly reduce the transfer limitation for the biomolecules.

Expansion characteristics

The expansion characteristics of the composite particles are shown in Figures 11(a) and 11(b). For two size fractions, it was found that the expansion factor decreased obviously with the increase of Ni-powder amount in the composite particles. For the particles with wet density of 1.6–1.8 g/mL, the bed could be operated at the fluid velocity of 1200 cm/h. The bed expansion of Cell-Ni-S was higher than that of the Cell-Ni-L because of lower density under same fluid velocity and the ratio of Ni-powder/viscose. The result indicated that the small fraction Cell-Ni-S could be used for varying flow velocity, from 300 to 1200 cm/h, with the expansion factor of 2–3 for different ratio of Ni-powder/viscose, while the large fraction Cell-Ni-L could be used for high flow velocity and relatively fast adsorption process. Particularly, the expansion factor of Cell-Ni-S4 was similar to that of Streamline Direct CST-1, for the expansion degree of 2.5 at 600 cm/h and 3 at 800 cm/h.

The expansion behaviors were correlated with flow velocity by the Richardson-Zaki equation [Eq. (6)]. As shown in Figures 12(a) and 12(b), good linear relations between the expansion voidage and flow velocity was found for all matrices tested. The correlated parameters of U_t and n are listed in Table I. It could be found that the values of n changed slightly at the range of 4.3–4.8 for Cell-Ni-S and 4.3–5.0 for Cell-Ni-L. The values of U_t increased significantly with the increase of particles densities.

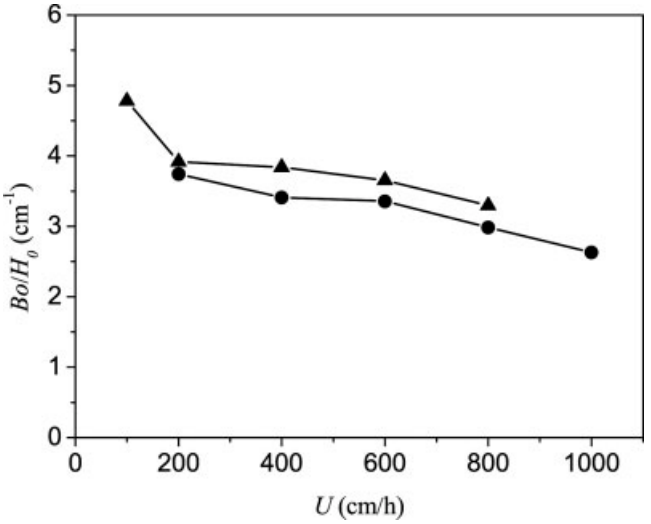

Figure 13 *Bo* number as the function of flow velocity: ▲, Cell-Ni-S4; ●, Cell-Ni-L4.

Liquid mixing in expanded bed for Cell-Ni-S4 and Cell-Ni-L4

The RTD tests with Cell-Ni-S4 and Cell-Ni-L4 were carried out to evaluate the liquid mixing in expanded bed. The Bodenstein number, *Bo*, was calculate with Eqs. (9) and (10) and the results are shown in Figure 13. The parameter of Bo/H_0 was used in the present work is to eliminate the influence of different initial bed height. The values of Bo/H_0 ranged from 3.3 to 4.8 cm^{-1} for Cell-Ni-S4 and 2.6 to 3.7 cm^{-1} for Cell-Ni-S4, and decreased with the increase of flow velocity. It could be found that the expanded bed with Cell-Ni-S4 is more stable than that with Cell-Ni-L4. The axial mixing coefficients D_{ax} were also calculated with Eq. (8). As shown in Figure 14, the values of D_{ax} increased obviously with the increasing of flow veloc-

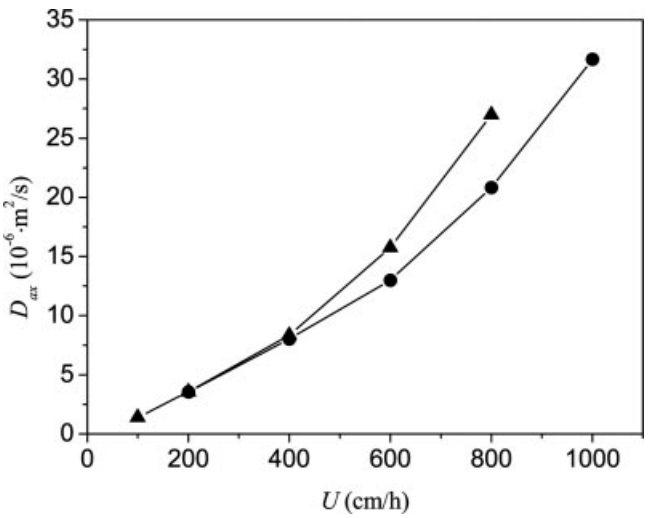

Figure 14 Axial mixing coefficient (D_{ax}) as the function of flow velocity: ▲, Cell-Ni-S4; ●, Cell-Ni-L4.

ity, which meant that the bed stability would be influenced by the high flow velocity. The values of D_{ax} were less than 1.0×10^{-5} m^2/s for the flow velocity lower than 400 cm/h. Even for high flow velocity, the values of D_{ax} were 1.2×10^{-5} m^2/s at the flow velocity of 500 cm/h (corresponding the expanded factor of 2.5) for Cell-Ni-S4, and 2.7×10^{-5} m^2/s at the flow velocity of 900 cm/h (corresponding the expanded factor of 2) for Cell-Ni-L4. The results demonstrated that the composite particles prepared in the present could form a stable fluidized bed for EBA application.

CONCLUSIONS

The spherical cellulose-nickel powder composite particles were prepared through the method of water-in-oil suspension thermal regeneration. Two fractions of composite particles with mean sizes of 101–119 μm and 168–217 μm were obtained. The cellulose–nickel powder composite particles prepared have the spherical appearance, suitable size and size distribution, appropriate wet density of 1.14–1.78 g/mL, water content of 51–75%, porosity of 81–93%, pore radius of 41–59 nm, and specific surface area of 30–42 m^2/mL of wet particles. The effects of nickel powder addition on the physical properties of the composite particles were analyzed. In addition, the bed expansions were investigated under varying flow rates, which indicated that the composite particles were suitable for high velocity operation. The expansion behaviors could be described by the Richardson-Zaki equation. The RTD measurements were used to evaluate the bed stability. Two important factors, *Bo* and D_{ax}, were analyzed to describe the liquid mixing in expanded bed. The results demonstrated that the composite particles prepared could form a stable fluidized bed and have a potential to use as the matrices for EBA applications.

The support of the National Natural Science Foundation of China is gratefully acknowledged. The authors also want to thank the German Academic Exchange Service (DAAD) for the instrument donation of Spectrophotometer K2600 and GE Healthcare for the kind gift of Streamline Direct CST-1.

References

1. Hjorth, R. Trends Biotechnol 1997, 15, 230.
2. Anspach, F. B.; Curbelo, D.; Hartmann, R.; Garke, G.; Deckwer, W.-D. J Chromatogr A 1999, 865, 129.
3. Hubbuch, J.; Thömmes, J.; Kula, M.-R. Adv Biochem Eng Biotechnol 2005, 92, 101.
4. Hamilton, G. E.; Luechau, F.; Burton, S. C.; Lyddiatt, A. J Biotechnol 2000, 79, 103.
5. Thömmes, J. Adv Biochem Eng Biotechnol 1997, 58, 185.
6. Amersham Biosciences, Uppsala, Sweden. Available at http://www.amershambiosciences.com.
7. Tong, X. D.; Sun, Y. J Chromatogr A 2002, 943, 63.
8. UpFront Chromatography A/S, Copenhagen, Denmark. Available at http://www.upfront-dk.com.
9. Zhou, X.; Shi, Q. H.; Bai, S.; Sun, Y. Biochem Eng J 2004, 18, 81.
10. Lei, Y. L.; Lin, D. Q.; Yao, S. J.; Zhu, Z. Q. J Appl Polym Sci 2003, 90, 2848.
11. Miao, Z. J.; Lin, D. Q.; Yao, S. J. Ind Eng Chem Res 2005, 44, 8218.
12. Gemeiner, P.; Benes, M. J.; Stamberg, J. Chem Pap 1989, 43, 805.
13. Kaewprasit, C.; Hequet, E.; Abidi, N.; Gourlot, J. P. J Cotton Sci 1998, 2, 164.
14. He, B. L.; Huang, W. Q. Ion Exchange and Adsorbent Resins; Shanghai Scientific and Technological Education Publishing House: Shanghai, China, 1992.
15. Richardson, J. F.; Zaki, W. N. Trans Inst Chem Eng 1954, 32, 35.
16. Thömmes, J.; Bader, A.; Halfar, M.; Karau, A.; Kula, M. R. J Chromatogr A 1996, 752, 111.
17. Lin, D.-Q.; Miao, Z.-J.; Yao, S.-J. J Chromatogr A 2006, 1107, 265.